Pharm Res (2013) 30:2709–2717
DOI 10.1007/s11095-013-1110-8

EXPERT REVIEW

MRI-Guided Monitoring of Thermal Dose and Targeted Drug Delivery for Cancer Therapy

Ruchika Fernando • Jon Downs • Danny Maples • Ashish Ranjan

Received: 13 February 2013 / Accepted: 4 June 2013 / Published online: 19 June 2013

ABSTRACT Application of localized hyperthermia treatment for solid tumor therapy is under active clinical investigation. The success of this treatment methodology, whether for tumor ablation or drug delivery, requires accurate target localization and real-time temperature mapping of the targeted region. Magnetic Resonance Imaging (MRI) can monitor temperature elevations in tissues in real-time during tumor therapy. MRI can also be applied in concert with methods such as High Intensity Focused Ultrasound (HIFU) to enable image-guided drug delivery (IGDD) from temperature sensitive nanocarriers, by exploiting not only its anatomic resolution, but its ability to detect and measure drug release using markers co-loaded with drugs within the nanocarriers. We review this rapidly emerging technology, providing an overview of MRI-guided tissue thermal dose monitoring for HIFU and Laser therapy, its role in targeted drug delivery and its future potential for clinical translation.

KEY WORDS Targeted drug delivery · nanoparticles · MRI thermal mapping · HIFU · Laser

INTRODUCTION

The earliest description of medical use of hyperthermia treatment of tumor was found in a 5,000 year-old Egyptian papyrus (1). Today, localized mild hyperthermia (40–42°C) or ablative therapy (>60°C) is often combined with chemotherapy or radiotherapy to achieve additive or synergistic killing of cancer cells (2,3). Available applicator technologies for producing localized hyperthermia in tumors include High Intensity Focused Ultrasound (HIFU), laser, radiofrequency ablation, and microwave irradiation (4–7). Despite significant advances in these methods, however, their abilities to provide spatially accurate and deep hyperthermia in solid tumors are often limited. To address these shortcomings, ultrasound- and laser-based hyperthermia applicators are being combined with Magnetic Resonance Imaging (MRI) to achieve integrated MRI-guided thermal therapy (8–10). This approach uses MRI to acquire anatomic images for targeted treatment planning, and to perform accurate temperature imaging for treatment monitoring and control. Such MRI-guided thermal therapy provides more precise and consistent thermal therapy in the target tissues, where its biological-effects are highly dependent on exposure times and temperatures.

The temporal and thermometric precision of MRI-guided local hyperthermia has also been harnessed to enable Image Guided Drug Delivery (IGDD) (11,12). IGDD is a highly interdisciplinary technology that integrates the principles of chemotherapy and imaging to achieve "personalized medicine", the goals of which are to devise patient-centered efficacious, individualized chemotherapeutic interventions (13). The process for developing such personalized therapies may incorporate patient information acquired from *ex vivo* or *in vivo* studies and responses to treatment (13). In this connection, real-time imaging offers tremendous advantages for developing personalized therapies, by providing feedback that allows active monitoring of drug delivery, release, and responses to therapy (11). Available imaging technologies that can be used to visualize responses to treatment include ultrasound, computed tomography (CT), and MRI. Here we first provide an overview of the uses and limitations of the available platforms for real-time thermometry, induction of localized hyperthermia or ablative tissue heating, and assessing responses to treatment. We then

R. Fernando · J. Downs · D. Maples · A. Ranjan
Laboratory of Nanomedicine & Targeted Therapy
Department of Physiological Sciences Oklahoma State University
Stillwater, Oklahoma, USA

A. Ranjan (✉)
169 McElroy Hall, Physiological Sciences
Center for Veterinary Health Sciences
Stillwater, Oklahoma, USA
e-mail: ashish.ranjan@okstate.edu

review emergent IGDD technologies, focusing on those that utilize MRI-guided localized hyperthermia to activate chemotherapeutic drug release from nanocarriers, in order to deliver selectively-targeted solid tumor therapy.

ROLE OF MRI IN TISSUE THERMAL DOSE MONITORING

A key prerequisite to achieving reliable and efficacious temperature-triggered drug delivery for clinical use is the need for accurately controlled non-invasive localized heating of target tissues (14). The need for such technology has been a limiting factor and persistent challenge to the advancement of IGDD-based therapies. Critical to achieving such fine control of tissue heating is a need for accurate temperature maps, which can permit controlled heating of target areas while minimizing adverse effects on neighboring tissues during treatment. MRI is an imaging procedure employing strong magnetization of nuclei, and that has been heavily investigated as a reliable way to generate thermal maps, while also providing superior tissue contrast compared with those provided by other imaging techniques used to guide drug delivery (12,14–16).

The use of MRI in thermotherapy depends on manipulating the temperature-dependent parameters; including Proton Resonance Frequency (PRF), T_1 and T_2 relaxation times, the diffusion coefficient, and temperature-sensitive contrast agent (17). T_1 (spin lattice relaxation time) describes how long an excited proton takes to revert to its original state. Within a small temperature range, T_1 varies linearly with temperature (16,18). Most tissues exhibit temperature dependence on the order of 1% per °C, but the coefficient of each tissue is distinct, and local factors influence it, and thereby affect T1-based MRI thermometry (16). In contrast, diffusion MRI is based on the assumption that water molecules move randomly unless compartmentalized by constraining structures such as cells (17), and changes in diffusion can thus be used to generate gradient maps. For example, during treatment of brain tumor, the decreased water compartmentalization (resulting from cell destruction) causes higher diffusion values detectable by MRI (19,20).

Another method that has recently gained prominence for guiding treatment from laser- and HIFU-based heat deposition is Proton Resonance Frequency Shift (PRFS) thermometry (21–23). PRFS allows high spatial and temporal resolution, and thereby potentially improved thermal therapy. The PRF of a given nucleus is determined by the local magnetic field acting upon it. The chemical phase of PRF depends both on temperature-dependent and -independent factors, but the former vary linearly within a small temperature range (16). Therefore, the proportional temperature change between one phase-shift image and another can be estimated accurately by computing their difference and factoring out temperature independent (i.e. constant) values. The PRF method involves certain limitations. First, it assumes no temperature dependence of the magnetic susceptibility. However, adipose tissues do exhibit some degree of temperature dependent susceptibility. Aqueous tissues likewise exhibit some temperature-dependence, but to a lesser, more predictable extent (16), and the PRF of water (~0.01 ppm/°C) is largely independent of aqueous tissue type (17). Methods are available for correcting variability attributable to the presence of adipose by suppressing contribution of lipid to the phase image, thereby permitting generation of reasonably accurate temperature maps (22). Second, because the error rate of measured temperature (dT) is the inverse of the signal to noise ratio, it is influenced by echo time within the targeted region (16,17). Despite these various considerations and limitations, if the assumptions are appropriately addressed, all of the MRI thermometry methods permit acquisition of accurate images of anatomical structures and tumor targets for planning treatments, and of thermometric maps to achieve the desired biological effects of thermal therapy and IGDD in target tissues. Below we discuss the application of MRI-thermometry in IGDD focusing mainly on HIFU-mediated release from temperature sensitive liposomes and laser directed ablative and photothermal therapy of solid tumor.

MRI AND HIFU (MRI-HIFU) COMBINATION FOR IGDD

MRI has been combined with HIFU in order to permit anatomically selective IGDD, elevating target tissue temperature while minimizing effects on non-targeted areas, guided by thermal mapping. Such combined MRI-HIFU combination has advanced markedly during the last decade for loco-regional therapy of solid tumors. In this approach the ultrasound transducer delivers focused high-frequency (orders of magnitude higher than those used for imaging) mechanical sound waves to patient tissues, causing a rise and fall of tissue pressure, and generating heat locally in the tissue (24–26). Early HIFU instrument designs employed single-element, spherical-shell transducers, which allowed heating that was restricted to an elliptical focal point only few millimeters in diameter using MHz-range frequency. Next generation HIFU applicators used mechanical displacement of the transducer to permit heating of larger regions (26). Although superior, the mechanical-displacement approach introduced additional limitations. First, it can affect the homogeneous heating of the tissues due to the rapid temperature distribution around the focal point. Second, phase perturbation may occur due to variations in the magnetic field caused by the mechanical movement.

To circumvent these problems, MRI-compatible stationary, multiple single-element phased array transducers are now used (25,27). These allow rapid heating of larger tissue volumes, either by splitting the natural focus into concurrent

multiple foci (28–30) or by constantly switching between preset multi-foci patterns during heating, eliminating the need for transducer movement (31,32). Desired focal pattern are produced by precisely adjusting the relative phase of the acoustic waves generated by each element of the phased-array transducers. Nevertheless, phased-array HIFU transducers do have technical limitations. First, heating multiple simultaneous focal points can generate heat lobes located outside the intended tissue area (33), particularly along the beam axis during heating of larger volume trajectories. For example, without careful correction, the center of a 12 mm^3 treatment volume may be up to ~0.5°C warmer than its periphery (9). Such limitations can be mitigated to a large extent by adjusting power, or modifying focus geometry and transducer. Further technology developments will likely continue to improve conformal heating *via* HIFU, in order to further protect tumor-adjoining healthy tissue.

Selective tissue heating *via* combined MRI-HIFU approaches is the subject of continuing investigation, but they are already used in a variety of pre-clinical applications including: 1) loco-regional release of drugs (8,10,34,35), and 2) inducing/reporting extravasation of drug-laden nanocarriers to enhance cellular uptake (34,36,37).

Liposomal Drug Nanocarriers Used with MRI-HIFU for IGDD

A major area of translational advance enabled by MRI-HIFU guided hyperthermia has been *via* combination with liposomes for IGDD. The concept of liposomes as a lipid bilayer enveloping an aqueous compartment was developed by A.D. Bangham and colleagues in *1965 (*38). This architecture is advantageous in conferring ability to transport hydrophilic drugs, which can be incorporated into the aqueous compartment, and the hydrophobic drugs, which can be incorporated into the lipid bilayer (39). The discovery of temperature-sensitive liposomes (TSLs) by Yatvin and Weinstein during the late 1970s conferred further targeting selectivity, that is now widely exploited through combination with MRI-HIFU (40,41). The driving principle of TSL drug delivery is as follows. Encapsulation of drugs in TSLs with appropriate temperature-activation thresholds prevents their extravasation into healthy tissue at normal body temperature. When the melting phase transition temperature (Tm) of the TSL lipid bilayer is reached during externally-induced heating of the targeted (i.e. tumor) tissue, the encapsulated drugs are released, providing potentially exquisite selective drug delivery to target tissues while minimizing systemic exposure to the TSL-encapsulated chemotherapeutic or other agents, thus minimizing adverse side effects (42–46).

The concept of hyperthermia-triggered drug delivery using TSLs has been tested in combination with various heating modalities, including immersion in water baths, needle-based radiofrequency catheters, light sources, microwaves and laser techniques, in addition to HIFU (46–50). For example, immersing body region that contains a targeted tissue in a warm water bath (~43°C) can achieve core tumor temperatures of 41–42°C. This can be used selectively to induce drug release from TSLs in experimental settings, such as study of a tumor bearing leg of a mouse, or a patient's arm or leg. However, this approach is obviously limited by its physically cumbersome nature and lack of fine, tumor-selective anatomic control of tissue heating. Below we describe alternatives that have been explored to circumvent this problem.

Greater tumor-specific hyperthermia was achieved in canine solid tumors using a clinically-relevant scanning annular phased-array microwave applicator applied between 140 and 433 mHz. Hyperthermia was maintained for a total of 30 min, and was continued for 1 h after the TSL infusion ended, monitored by temperature probes inserted in tumor. The median T_{50} achieved over all given hyperthermia treatments was 41.22°C (range, 37.38–44.03°C). Additionally, TSLs have been combined with ultrasound guided, pulsed high intensity focused ultrasound (pulsed-HIFU) for enhanced antitumor effects in a murine mammary adenocarcinoma tumor model (51,52). In these studies, mouse tumors were first aligned with transducer's focal zone, and pulsed-HIFU was applied for 15–20 min to achieve local hyperthermia (42 ± 4°C) in the entire tumor volume. Similar to the microwave study, the temperature in a non-exposed region of the tumor, and in the exposed region were measured simultaneously, in real time, using fluorometric thermocouples. The results showed an increase in temperature and stabilization of the peak temperature during the HIFU exposure. Although advantageous compared to water bath heating, microwave and pulsed HIFU applicators in the absence of real-time thermal mapping are limited in their ability to provide a spatially accurate or deep thermal therapy to a solid tumor. Thus, to provide a more consistent treatment, MRI-HIFU due to its ability to provide non-invasive deep tissue hyperthermia and accurate spatio-temporal thermal mapping in tumors is presently the most effective means for achieving controlled IGDD, as illustrated below (Fig. 1).

In one MRI-HIFU drug delivery study in rabbits, temperature maps were obtained using the PRFS method, and the mean temperature of the target tissue was maintained uniformly by a binary feedback algorithm (34). A 4 mm region within a tumor of each rabbit was heated, in intervals of up to 10 min each that began immediately after administration of doxorubicin-loaded TSL by using an electronically-steered HIFU beam that moved in a circular trajectory immediately (Fig. 2). Intratumoral doxorubicin levels within the MRI-HIFU-treated tissue were increased by 3–4 compared with those seen in non-heated tumors, and 8 fold *versus* those seen in tumors of rabbits that were treated with free doxorubicin. Similar studies conducted elsewhere revealed 2-17 fold higher intratumoral doxorubicin concentrations delivered by TSL

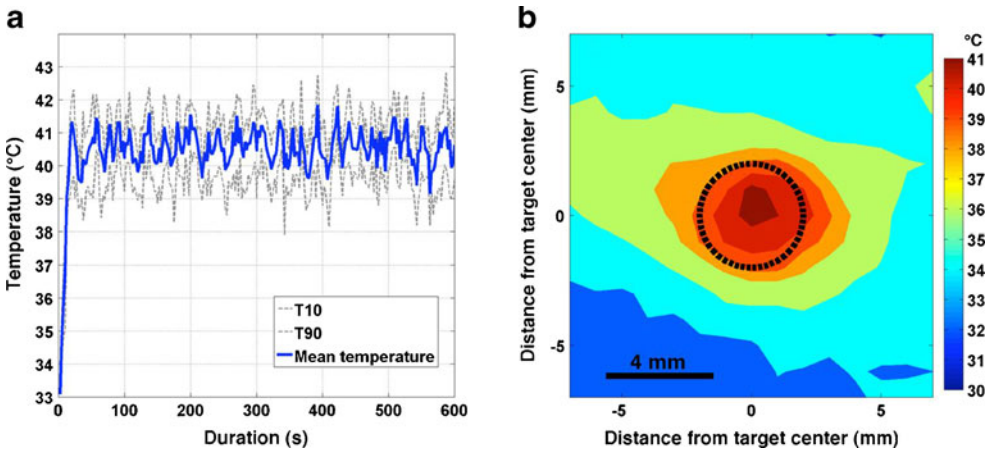

Fig. 1 Illustrates temperature elevation and spatial distribution of heat during HIFU sonication. (**a**) Shows the stable mild hyperthermia achieved in the tumor/target by precisely controlling HIFU power, mediated through a binary feedback control based on the real time target temperature. (**b**) Time averaged spatial distribution of temperature in the target region (*black circle*) and the surrounding tissue, showing a uniformity of elevated temperature in the target region.

accompanied by MRI-HIFU compared to those seen without tissue heating depending on tissue type (34,51,53). For example, when 10-15 mm diameter regions within the rabbit thigh was heated to 43°C for 20 min immediately after TSL infusion, drug concentrations in the heated regions was shown to be about 15.8 times higher than in the corresponding unheated regions of the contralateral thigh (53). In contrast, IGDD in bones with a similar hyperthermia protocol (43°C, 20 min) protocol demonstrated 8.2-fold greater doxorubicin concentration in heated *versus* unheated bone marrow (35).

Enhancement of Intratumoral Drug Distribution by MRI-HIFU

Intratumoral delivery of chemotherapeutic drugs (*e.g.* doxorubicin) *via* TSL has been assessed by image analysis of fluorescence intensity (8,34,36). For example, after administration of doxorubicin-containing TSL followed by MRI-HIFU, fluorescence intensity indicative of intratumoral doxorubicin (Fig. 3) concentrations was elevated in the tumor periphery as well as its core, as compared with that seen in tumors of rabbits treated with doxorubicin alone, or with doxorubicin-loaded LTSL without MR-HIFU heating. Such enhanced intratumoral drug distribution in the tumor core was similarly attained upon sonication of 10 mm diameter regions continuously to 43°C with a mechanically-steered MRI-guided spherically-focused ultrasound system transducer (curvature radius, 10 cm; aperture diameter, 5 cm) (8). These trends are similarly observed in rodent model. When hyperthermia was administered in rats bearing a subcutaneous rhabdomyosarcoma tumor on the hind leg using a clinical 3-Tesla MRI-HIFU system, the delivered drug was spread over a much larger area in the in the HIFU-treated tumors *versus* unheated tumors (36). Aside from heat-induced drug release from TSL used in concert with MRI-HIFU, an additional mechanism that may further enhance drug distribution is thermoregulatory-mediated elevations of intratumoral blood flow (54). Local hyperthermia probably decreases resistance in vascular beds proximal and distal to the tumor vasculature throughout the tumor, perhaps in part by drawing excess fluid from tumor stroma and thereby relieving interstitial pressure, and decompressing tumor vasculature (55). Additionally, hyperthermia induces vessel normalization and improves tumor perfusion to the tumor core and can establish a high intravascular drug concentration leading to the improved drug coverage observed in heated tumor (56,57).

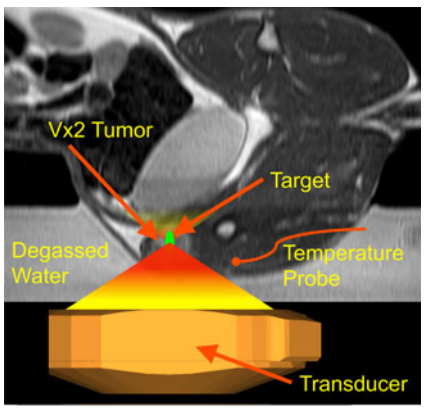

Fig. 2 Illustrates the basic MRI guided HIFU mediated hyperthermia setup. The target area (rabbit Vx2 tumor) is placed in a water bath, containing degassed water, directly under the 256-element, high intensity focused, phased array ultrasound transducer. Temperature maps were obtained using the PRFS method. The mean temperature of the target tissue was maintained uniformly by using a binary feedback algorithm on HIFU system where it applies heat when the mean tissue temperature is ≤40°C, and stops heating at 41°C.

Real-Time Monitoring of Intra-Tumor Drug Release by MRI in IGDD

In addition to its application for intratumoral drug delivery, combined application of MRI-HIFU with TSL is being utilized to report the drug level in tumors in real time to personalize drug dosage. For example, co-encapsulation of paramagnetic MRI contrast agents and anticancer drugs within TSL has shown to facilitate analysis of release kinetics.

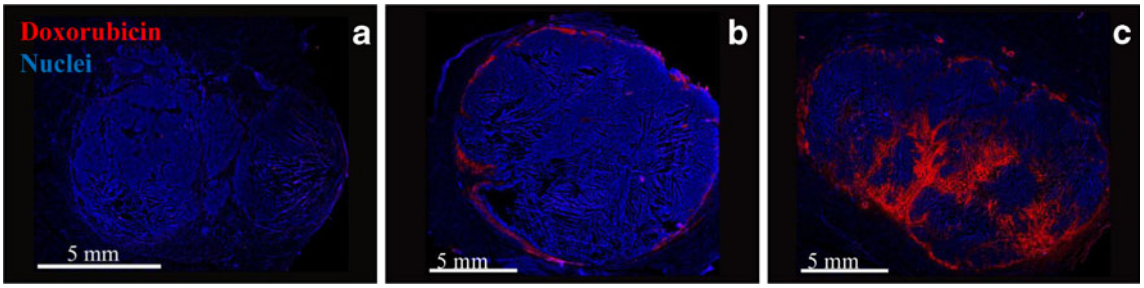

Fig. 3 Fluorescent images showing Dox distribution in the tumor following intravenous injection of free Dox (**a**) and LTSL-Dox (**b**) and LTSL-Dox in combination with MRI-HIFU heating (**c**) of the Vx2 tumors. The nuclei of the tumor cells are stained in *blue* and Dox is seen in bright *red* color. Free doxorubicin and LTSL treatments appeared to deliver more drugs in the tumor periphery as compared to the tumor core. In contrast, LTSL+MR-HIFU treatment suggest an improved distribution with doxorubicin found in both the tumor periphery and core.

TSLs have minimal permeability until phase-shift temperature is reached, at which point the permeability of TSL membrane increases allowing water to move more freely between the liposome and its surroundings (58). This allows the encapsulated contrast agent (usually a rare metal) to alter the relaxation time of molecules entering from the surroundings, which is detectable *via* MRI (59). The changes in MRI signal that occurs near the Tm of the TSL upon release of the contrast agents provides information that permits prediction and visualization of drug release. Real-time temperature-induced drug delivery under MRI image-guidance was first achieved using TSLs in which doxorubicin was co-encapsulated with manganese (Mn). Although Mn can serve adequately as a T1-weighted MRI contrast agent, it has not been developed for clinical use owing to its potential adverse side effect profile (50). Consequently, later-generation TSL approaches have substituted gadolinium (Gd), a clinically approved T1-weighted MRI contrast agent, co-loaded with doxorubicin (10,60).

Several examples of preclinical studies illustrate the advantages of this approach. Using Gd and doxorubicin co-encapsulated in TSLs, and a clinical MRI-HIFU system, real-time monitoring of TSL mediated doxorubicin delivery in rats bearing subcutaneous glioblastoma tumors was achieved (10). The HIFU system in this study contained a 256-element phased array transducer and a dedicated small-animal MRI coil fitted to the ultrasound transducer. The authors found good correlation between the change in longitudinal relaxation rate (the difference in T1 values averaged over the whole tumor before and after TSL injection), the uptake of doxorubicin, and the intra-tumoral gadolinium concentration, indicating that doxorubicin release from TSLs can be probed *in situ* using the longitudinal relaxation rates of the co-released Gd. Similar findings resulted when Gd release was analyzed in a rabbit tumor model, using a system that included a clinical 1.5 T MRI scanner and an electromechanically positioned phased array HIFU transducer containing 256-elements. Mild hyperthermia of tumors following Gd- and doxorubicin-co-loaded TSL administration revealed the greatest signal increase (30–60%) in the heated tumors (37), thereby demonstrating the feasibility of the real-time monitoring of intra-tumor drug release by MRI in IGDD (37). More recently, MRI provided monitoring of drug release in tumor-bearing mice from novel TSLs that contained only two components (DPPC/Brij78 in 96/4 molar ratio) *vs*. TSL (DPPC/MSPC/DSPE-PEG2000 in molar ratio of 85.3/9.7/5.0) (61). In addition to containing different lipid components compared to TSLs, these novels liposomes exhibit 1.2- to 2-fold increased drug release at 40–41°C compared to TSL. MRI in this study was performed using a 7-Tesla magnet. Analysis of average difference in T1 pre and post hyperthermia treatment revealed significantly increased T1 relaxation rates one hour after parenteral injection in heated tumors, thereby successfully predicting the therapeutic delivery. Overall, available evidence thus indicates that combined application of MRI-HIFU with TSL has significant translational potential, and addresses major shortcomings of conventional chemotherapeutic methods, by permitting selective intra-tumoral delivery of even nonselective standard chemotherapy agents, and real-time monitoring of such local drug delivery.

COMBINED USE OF MRI AND LASER COMBINATION FOR ABLATIVE AND IGDD-BASED TUMOR THERAPY

Role of MRI in Laser-Based Ablative Therapy

The use of laser therapy for surgical ablation of neoplastic tissues is widespread since late 1960s (62–64). Laser delivers high-energy radiation using optical fibers and can achieve ablative temperature (>60°C) elevation and coagulation necrosis within the tumor core or other targeted tissue. Laser is usually transmitted through an optical fiber for external surface targets or is applied by inserting the laser tip (interstitial therapy) into the tumor core (65–67). Examples of laser thermal therapy

applicators include neodymium–yttrium aluminum garnet (Nd–YAG, 1.06 μm) and CO2 laser (10.6 μm) applicators (68). Major challenge in laser therapy have included the need for accurate target localization and real-time temperature mapping during ablation therapy, and a lack of adequate tools for addressing these has hindered progress. MRI-guided laser-induced thermal therapy (*e.g.* SOMATEX, Germany) of soft-tissue tumors can address both of these shortcomings (69). These minimally invasive systems consists of percutaneous MRI-compatible cannulation needles and French double-tube thermo-stable protective catheters with internal cooling capability (Fig. 4) that can be placed in tumors under ultrasound or CT guidance (68). Internal cooling of the surface of the laser applicator allows uniform temperature distribution into deeper tissues layers. MRI thermometry for these procedures follows similar guidelines as for HIFU as described earlier, relying mostly on T1-weighted or PRF phase-difference techniques. Also similarly to HIFU, laser hyperthermia can treat large tumor volumes. This is achieved by applying several laser applicators simultaneously or by a pull-back procedure that relies on T1-weighted thermal imaging during treatment to enlarge regions of coagulation necrosis (68).

Application of Laser in MRI Guided Drug Delivery

As in the case of HIFU, selective focal heating and IGDD of tissue mass in targeted locations can be greatly improved by combining MRI-Laser with various photothermally (PT) activated agents (70–74). Exposure of PT agents to light photons, along with light-induced interaction of PT agents, causes absorption and subsequent decay of electronic excitation energy that increase its kinetic energy and produces tissue heating, thereby destroying cells (75). Examples of PT agents for ablation and IGDD applications include endogeneous chromophores in tissues (70,76,77), and exogenous agents such as indocyanine green (78), naphthalocyanines (79), and porphyrins. These exogenous PT dyes have highly efficient light-to-heat conversion, reducing the amount of light required to generate the desired level of heat with minimum invasiveness to neighboring tissues (75). Widely used nanoparticle PT agents include gold nanospheres (80,81), gold nanorods (82), gold nanoshells (83), gold nanocages (84), and carbon nanotubes (85). All of these nanoparticles provide a superior absorption of visible and NIR light, and can generate hyperthermia for killing cancer cells (83). Such nanoparticles are also advantageous because they exhibit less photobleaching than PT dyes (86). Addition of PT agents for IGDD is important clinically, because hyperthermia outcomes in tissue can vary based on thermal conductivity, diffusion, and physiological cooling effects. Combination of PT with MRI thermometry provides real-time guidance that can achieve desirable treatment benefits in a tightly-controlled fashion (87). PT agents can also be combined with polymer-based drug delivery system to further improve MRI guided drug delivery. For example, near-infrared (NIR) laser and hollow gold nanospheres (HAuNS) released paclitaxel (PTX) from poly(lactide-co-glycolide) (PLGA) copolymers in an *in vivo* mouse tumor model (88). The cumulative release of paclitaxel was found to be 40% when exposed to the NIR laser in presence of HAuNS. In contrast, without NIR the polymer-PTX conjugate released <7% of the of paclitaxel cargo during the same interval. Thus, MRI-Laser guided thermal therapy and PT agent combination has a tremendous role in future IGDD and oncologic therapy.

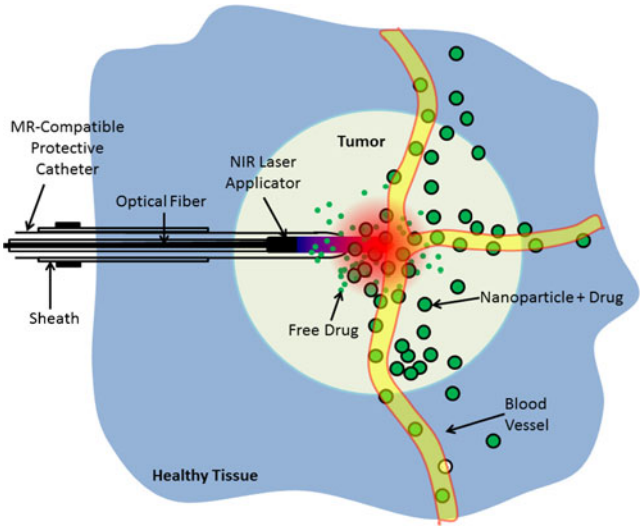

Fig. 4 Illustrates the laser induced IGDD set-up. The laser applicator is inserted into the tumor through an MRI-compatible protective catheter under image guidance. Nanoparticles (*e.g.* PLGA) shown in the figure are co-encapsulated with a drug (*e.g.* PTX) and PTT agent (*e.g.* gold nanoparticles). NIR laser generates heat in the presence of the PTT agent, and releases the drug from the nanoparticles. Temperature elevation in the tumor is monitored by MRI thermometry to avoid damage to adjoining healthy tissue.

CONCLUSION

Applied local hyperthermia of tumors for any treatment modality requires precise targeting to the intended site. This can be achieved by utilizing MRI, a single technology which uniquely provides 3 major capabilities: acquisition of anatomic targets structure for treatment planning, accurate thermometry for treatment monitoring and control, and real-time monitoring of intratumoral drug release. Although the technology is still in its infancy, MRI-guided hyperthermia and nanoparticles have been efficiently combined in preclinical studies for IGDD. To realize the full benefit of this combined therapeutic modality, individual patient's tumor physiology and trans-vascular transport properties would best be analyzed quantitatively prior to treatments using DCE-MRI, hypoxia, metabolism and ADC maps (89).

These combined and evolving technologies will significantly advance development of personalized solid tumor therapies matched to individual patient needs. Currently, hyperthermia treatment is generally achieved by a volumetric (concentric) approach. However, successful IGDD or even ablative therapy will eventually require large volume conformal hyperthermia in order to capture their full potential for loco-regional tumor therapy. Image guided tumor thermal therapy has strong translational potential for eventual routine clinical application, and improvements in patients' long-term survival and quality of life. IGDD in particular has rich potential for achieving these goals, and will continue to be a productive area for translational research to improve and advance the standard of care for solid tumor therapy.

REFERENCES

1. C. Sturesson, Lund A. Theoretical modeling of the temperature distribution in laser-induced hyperthermia. Lund Reports on Atomic Physics (LRAP-159).1994.
2. van der Zee J, González D, van Rhoon GC, van Dijk JDP, van Putten WLJ, Hart AAM. Comparison of radiotherapy alone with radiotherapy plus hyperthermia in locally advanced pelvic tumours: a prospective, randomised, multicentre trial. Lancet. 2000;355:1119–25.
3. Kitamura K, Kuwano H, Watanabe M, Nozoe T, Yasuda M, Sumiyoshi K, *et al.* Prospective randomized study of hyperthermia combined with chemoradiotherapy for esophageal carcinoma. J Surg Oncol. 1995;60:55–8.
4. Napoli A, Anzidei M, Ciolina F, Marotta E, Cavallo Marincola B, Brachetti G, *et al.* MR-guided high-intensity focused ultrasound: current status of an emerging technology. Cardiovasc Interv Radiol. 2013.
5. Oto A, Sethi I, Karczmar G, McNichols R, Ivancevic MK, Stadler WM, *et al.* MR imaging-guided focal laser ablation for prostate cancer: phase I trial. Radiology. 2013.
6. Shah DR, Green S, Elliot A, McGahan JP, Khatri VP. Current oncologic applications of radiofrequency ablation therapies. World J Gastrointest Oncol. 2013;5:71–80.
7. Swan RZ, Sindram D, Martinie JB, Iannitti DA. Operative microwave ablation for hepatocellular carcinoma: complications, recurrence, and long-term outcomes. J Gastrointest Surg. 2013;17:719–29.
8. Staruch RM, Ganguly M, Tannock IF, Hynynen K, Chopra R. Enhanced drug delivery in rabbit VX2 tumours using thermosensitive liposomes and MRI-controlled focused ultrasound hyperthermia. Int J Hyperther. 2012;28:776–87.
9. Partanen A, Yarmolenko PS, Viitala A, Appanaboyina S, Haemmerich D, Ranjan A, *et al.* Mild hyperthermia with magnetic resonance-guided high-intensity focused ultrasound for applications in drug delivery. Int J Hyperth. 2012;28:320–36.
10. de Smet M, Heijman E, Langereis S, Hijnen NM, Grull H. Magnetic resonance imaging of high intensity focused ultrasound mediated drug delivery from temperature-sensitive liposomes: an in vivo proof-of-concept study. J Control Release. 2011;150:102–10.
11. Tandonand P, Farahani K. NCI image-guided drug delivery summit. Cancer Res. 2011;71:314–7.
12. Hynynen K. MRIgHIFU: a tool for image-guided therapeutics. J Magn Reson Imaging. 2011;34:482–93.
13. Lammers T, Rizzo LY, Storm G, Kiessling F. Personalized nanomedicine. Clin Cancer Res. 2012;18:4889–94.
14. Grülland H, Langereis S. Hyperthermia-triggered drug delivery from temperature-sensitive liposomes using MRI-guided high intensity focused ultrasound. J Control Release. 2012;161:317–27.
15. Leach MO. Breast cancer screening in women at high risk using MRI. NMR Biomed. 2009;22:17–27.
16. Quesson B, de Zwart JA, Moonen CTW. Magnetic resonance temperature imaging for guidance of thermotherapy. J Magn Reson Imaging. 2000;12:525–33.
17. Riekeand V, Butts Pauly K. MR thermometry. J Magn Reson Imaging. 2008;27:376–90.
18. Viglianti BL, Abraham SA, Michelich CR, Yarmolenko PS, MacFall JR, Bally MB, *et al.* In vivo monitoring of tissue pharmacokinetics of liposome/drug using MRI: illustration of targeted delivery. Magn Reson Med. 2004;51:1153–62.
19. Kopelman R, Lee Koo YE, Philbert M, Moffat BA, Ramachandra Reddy G, McConville P, *et al.* Multifunctional nanoparticle platforms for in vivo MRI enhancement and photodynamic therapy of a rat brain cancer. J Magn Magn Mater. 2005;293:404–10.
20. Chenevert TL, Stegman LD, Taylor JM, Robertson PL, Greenberg HS, Rehemtulla A, *et al.* Diffusion magnetic resonance imaging: an early surrogate marker of therapeutic efficacy in brain tumors. J Natl Cancer Inst. 2000;92:2029–36.
21. Salomir R, Vimeux FC, de Zwart JA, Grenier N, Moonen CT. Hyperthermia by MR-guided focused ultrasound: accurate temperature control based on fast MRI and a physical model of local energy deposition and heat conduction. Magn Reson Med. 2000;43:342–7.
22. de Zwart JA, Vimeux FC, Delalande C, Canioni P, Moonen CT. Fast lipid-suppressed MR temperature mapping with echo-shifted gradient-echo imaging and spectral-spatial excitation. Magn Reson Med. 1999;42:53–9.
23. de Senneville BD, Mougenot C, Moonen CT. Real-time adaptive methods for treatment of mobile organs by MRI-controlled high-intensity focused ultrasound. Magn Reson Med. 2007;57:319–30.
24. Chen L, Rivens I, Ter Haar G, Riddler S, Hill CR, Bensted JPM. Histological changes in rat liver tumours treated with high-intensity focused ultrasound. Ultrasound Med Biol. 1993;19:67–74.
25. Hynynen K, Roemer R, Anhalt D, Johnson C, Xu ZX, Swindell W, *et al.* A scanned, focused, multiple transducer ultrasonic system for localized hyperthermia treatments. Int J Hyperth. 1987;3:21–35.
26. Hynynen K, Freund WR, Cline HE, Chung AH, Watkins RD, Vetro JP, *et al.* A clinical, noninvasive, MR imaging-monitored ultrasound surgery method. Radiographics. 1996;16:185–95.
27. Lin WL, Chen YY, Lin SY, Yen JY, Shieh MJ, Kuo TS. Optimal configuration of multiple-focused ultrasound transducers for external hyperthermia. Med Phys. 1999;26:2007.
28. Ebbini ES, Cain CA. Multiple-focus ultrasound phased-array pattern synthesis: optimal driving-signal distributions for hyperthermia. IEEE Trans Ultrason Ferroelectr Freq Control. 1989;36:540–8.
29. Fanand X, Hynynen K. Control of the necrosed tissue volume during noninvasive ultrasound surgery using a 16-element phased array. Med Phys. 1995;22:297.
30. Fanand X, Hynynen K. Ultrasound surgery using multiple sonications—treatment time considerations. Ultrasound Med Biol. 1996;22:471–82.
31. Daum DR, Hynynen K. Thermal dose optimization via temporal switching in ultrasound surgery. IEEE Trans Ultrason Ferroelectr Freq Control. 1998;45:208–15.
32. Daum DR, Hynynen K. A 256-element ultrasonic phased array system for the treatment of large volumes of deep seated tissue. IEEE Trans Ultrason Ferroelectr Freq Control. 1999;46:1254–68.
33. Köhler MO, Mougenot C, Quesson B, Enholm J, Le Bail B, Laurent C, *et al.* Volumetric HIFU ablation under 3D guidance of rapid MRI thermometry. Med Phys. 2009;36:3521.

34. Ranjan A, Jacobs GC, Woods DL, Negussie AH, Partanen A, Yarmolenko PS, *et al.* Image-guided drug delivery with magnetic resonance guided high intensity focused ultrasound and temperature sensitive liposomes in a rabbit Vx2 tumor model. J Control Release. 2012;158:487–94.
35. Staruch R, Chopra R, Hynynen K. Hyperthermia in bone generated with MR imaging-controlled focused ultrasound: control strategies and drug delivery. Radiology. 2012;263:117–27.
36. de Smet M, Hijnen NM, Langereis S, Elevelt A, Heijman E, Dubois L, *et al.* Magnetic resonance guided high-intensity focused ultrasound mediated hyperthermia improves the intratumoral distribution of temperature-sensitive liposomal doxorubicin. Investig Radiol. 2013;48:395–405.
37. Negussie AH, Yarmolenko PS, Partanen A, Ranjan A, Jacobs G, Woods D, *et al.* Formulation and characterisation of magnetic resonance imageable thermally sensitive liposomes for use with magnetic resonance-guided high intensity focused ultrasound. Int J Hyperth. 2011;27:140–55.
38. Bangham AD, Standish MM, Weissmann G. The action of steroids and streptolysin S on the permeability of phospholipid structures to cations. J Mol Biol. 1965;13:253–9.
39. Koningand GA, Krijger GC. Targeted multifunctional lipid-based nanocarriers for image-guided drug delivery. Anti Cancer Agents Med Chem. 2007;7:425–40.
40. Yatvin MB, Weinstein JN, Dennis WH, Blumenthal R. Design of liposomes for enhanced local release of drugs by hyperthermia. Science (New York, NY). 1978;202:1290–3.
41. Weinstein JN, Magin RL, Yatvin MB, Zaharko DS. Liposomes and local hyperthermia: selective delivery of methotrexate to heated tumors. Science. 1979;204:188–91.
42. Evansand E, Needham D. Physical properties of surfactant bilayer membranes: thermal transitions, elasticity, rigidity, cohesion and colloidal interactions. J Phys Chem. 1987;91:4219–28.
43. Anyarambhatlaand GR, Needham D. Enhancement of the phase transition permeability of DPPC liposomes by incorporation of MPPC: a new temperature-sensitive liposome for use with mild hyperthermia. J Liposome Res. 1999;9:491–506.
44. Leidy C, Wolkers WF, Jørgensen K, Mouritsen OG, Crowe JH. Lateral organization and domain formation in a two-component lipid membrane system. Biophys J. 2001;80:1819–28.
45. Veatch SL, Keller SL. Seeing spots: complex phase behavior in simple membranes. Biochim Biophys Acta (BBA) - Mol Cell Res. 2005;1746:172–85.
46. Kong G, Anyarambhatla G, Petros WP, Braun RD, Colvin OM, Needham D, *et al.* Efficacy of liposomes and hyperthermia in a human tumor xenograft model: importance of triggered drug release. Cancer Res. 2000;60:6950–7.
47. Viglianti BL, Ponce AM, Michelich CR, Yu D, Abraham SA, Sanders L, *et al.* Chemodosimetry of in vivo tumor liposomal drug concentration using MRI. Magn Reson Med. 2006;56:1011–8.
48. Needham D, Anyarambhatla G, Kong G, Dewhirst MW. A new temperature-sensitive liposome for use with mild hyperthermia: characterization and testing in a human tumor xenograft model. Cancer Res. 2000;60:1197–201.
49. Lindner LH, Eichhorn ME, Eibl H, Teichert N, Schmitt-Sody M, Issels RD, *et al.* Novel temperature-sensitive liposomes with prolonged circulation time. Clin Cancer Res. 2004;10:2168–78.
50. Ponce AM, Viglianti BL, Yu D, Yarmolenko PS, Michelich CR, Woo J, *et al.* Magnetic resonance imaging of temperature-sensitive liposome release: drug dose painting and antitumor effects. J Natl Cancer Inst. 2007;99:53–63.
51. Dromi S, Frenkel V, Luk A, Traughber B, Angstadt M, Bur M, *et al.* Pulsed-high intensity focused ultrasound and low temperature-sensitive liposomes for enhanced targeted drug delivery and antitumor effect. Clin Cancer Res. 2007;13:2722–7.
52. Frenkel V, Etherington A, Greene M, Quijano J, Xie J, Hunter F, *et al.* Delivery of liposomal doxorubicin (Doxil) in a breast cancer tumor model: investigation of potential enhancement by pulsed-high intensity focused ultrasound exposure. Acad Radiol. 2006;13:469–79.
53. Staruch R, Chopra R, Hynynen K. Localised drug release using MRI-controlled focused ultrasound hyperthermia. Int J Hyperth. 2010;27:156–71.
54. Vaupel P, Horsman MR. Tumour perfusion and associated physiology: characterization and significance for hyperthermia. Int J Hyperth. 2010;26:209–10.
55. Sen A, Capitano ML, Spernyak JA, Schueckler JT, Thomas S, Singh AK, *et al.* Mild elevation of body temperature reduces tumor interstitial fluid pressure and hypoxia and enhances efficacy of radiotherapy in murine tumor models. Cancer Res. 2011;71:3872–80.
56. Manzoor AA, Lindner LH, Landon CD, Park JY, Simnick AJ, Dreher MR, *et al.* Overcoming limitations in nanoparticle drug delivery: triggered, intravascular release to improve drug penetration into tumors. Cancer Res. 2012;72:5566–75.
57. Dings RP, Loren ML, Zhang Y, Mikkelson S, Mayo KH, Corry P, *et al.* Tumour thermotolerance, a physiological phenomenon involving vessel normalisation. Int J Hyperth. 2011;27:42–52.
58. Salomir R, Palussière J, Fossheim SL, Rogstad A, Wiggen UN, Grenier N, *et al.* Local delivery of magnetic resonance (MR) contrast agent in kidney using thermosensitive liposomes and MR imaging-guided local hyperthermia: a feasibility study in vivo. J Magn Reson Imaging. 2005;22:534–40.
59. Lindner L, Reinl H, Schlemmer M, Stahl R, Peller M. Paramagnetic thermosensitive liposomes for MR-thermometry. Int J Hyperth. 2005;21:575–88.
60. Hijnen NM, Heijman E, Köhler MO, Ylihautala M, Ehnholm GJ, Simonetti AW, *et al.* Tumour hyperthermia and ablation in rats using a clinical MR-HIFU system equipped with a dedicated small animal set-up. Int J Hyperth. 2012;28:141–55.
61. Tagami T, Foltz WD, Ernsting MJ, Lee CM, Tannock IF, May JP, *et al.* MRI monitoring of intratumoral drug delivery and prediction of the therapeutic effect with a multifunctional thermosensitive liposome. Biomaterials. 2011;32:6570–8.
62. N. Kapanyand N. Peppers. Retinal photocoagulatlon by lasers. 1963.
63. Minton JP, Carlton DM, Dearman JR, McKnight WB, Ketcham AS. An evaluation of the physical response of malignant tumor implants to pulsed laser radiation. Surg Gynaecol Obstet. 1965;121:538–44.
64. Ketcham AS, Hoye RC, Riggle GC. The laser in cancer research. Ann N Y Acad Sci. 1969;168:634–41.
65. Bown S. Phototherapy of tumors. World J Surg. 1983;7:700–9.
66. Steger A, Lees W, Walmsley K, Bown S. Interstitial laser hyperthermia: a new approach to local destruction of tumours. Br Med J. 1989;299:362–5.
67. Mastersand A, Bown S. Interstitial laser hyperthermia in tumour therapy. Ann Chir Gynaecol. 1990;79:244.
68. Vogl TJ, Naguib NNN, Lehnert T, Nour-Eldin NEA. Radiofrequency, microwave and laser ablation of pulmonary neoplasms: clinical studies and technical considerations—review article. Eur J Radiol. 2011;77:346–57.
69. Fuentes D, Walker C, Elliott A, Shetty A, Hazle JD, Stafford RJ. Magnetic resonance temperature imaging validation of a bioheat transfer model for laser-induced thermal therapy. Int J Hyperth. 2011;27:453–64.
70. Andersonand RR, Parrish JA. Selective photothermolysis: precise microsurgery by selective absorption of pulsed radiation. Science. 1983;220:524–7.
71. Parrish JA, Anderson RR, Harrist T, Paul B, Murphy GF. Selective thermal effects with pulsed irradiation from lasers: from organ to organelle. J Investig Dermatol. 1983;80:75s–80.

72. Welch A. The thermal response of laser irradiated tissue. IEEE J Quantum Electron. 1984;20:1471–81.
73. Joriand G, Spikes JD. Photothermal sensitizers: possible use in tumor therapy. J Photochem Photobiol B Biol. 1990;6:93–101.
74. Camerin M, Rello S, Villanueva A, Ping X, Kenney ME, Rodgers MAJ, *et al.* Photothermal sensitisation as a novel therapeutic approach for tumours: studies at the cellular and animal level. Eur J Cancer. 2005;41:1203–12.
75. Huang X, Jain PK, El-Sayed IH, El-Sayed MA. Plasmonic photothermal therapy (PPTT) using gold nanoparticles. Lasers Med Sci. 2008;23:217–28.
76. Rox Anderson R, Parrish JA. Microvasculature can be selectively damaged using dye lasers: a basic theory and experimental evidence in human skin. Lasers Surg Med. 2005;1:263–76.
77. Polla LL, Margolis RJ, Dover JS, Whitaker D, Murphy GF, Jacques SL, *et al.* Melanosomes are a primary target of Q-switch ruby laser irradiation in guinea pig skin. J Investig Dermatol. 1987;89:281–6.
78. Chen WR, Adams RL, Bartels KE, Nordquist RE. Chromophore-enhanced in vivo tumor cell destruction using an 808-nm diode laser. Cancer Lett. 1995;94:125–31.
79. Jori G, Schindl L, Schindl A, Polo L. Novel approaches towards a detailed control of the mechanism and efficiency of photosensitized processes in vivo. J Photochem Photobiol A Chem. 1996;102:101–7.
80. Pitsillides CM, Joe EK, Wei X, Anderson R, Lin CP. Selective cell targeting with light-absorbing microparticles and nanoparticles. Biophys J. 2003;84:4023–32.
81. Hainfeld JF, Slatkin DN, Smilowitz HM. The use of gold nanoparticles to enhance radiotherapy in mice. Phys Med Biol. 2004;49:N309.
82. Huang X, El-Sayed IH, Qian W, El-Sayed MA. Cancer cell imaging and photothermal therapy in the near-infrared region by using gold nanorods. J Am Chem Soc. 2006;128:2115–20.
83. Hirsch LR, Stafford R, Bankson J, Sershen S, Rivera B, Price R, *et al.* Nanoshell-mediated near-infrared thermal therapy of tumors under magnetic resonance guidance. Proc Natl Acad Sci. 2003;100:13549–54.
84. Chen J, Wiley B, Li ZY, Campbell D, Saeki F, Cang H, *et al.* Gold nanocages: engineering their structure for biomedical applications. Adv Mater. 2005;17:2255–61.
85. Kam NWS, O'Connell M, Wisdom JA, Dai H. Carbon nanotubes as multifunctional biological transporters and near-infrared agents for selective cancer cell destruction. Proc Natl Acad Sci U S A. 2005;102:11600–5.
86. Landsman M, Kwant G, Mook G, Zijlstra W. Light-absorbing properties, stability, and spectral stabilization of indocyanine green. J Appl Physiol. 1976;40:575–83.
87. Chen Y, Gnyawali SC, Wu F, Liu H, Tesiram YA, Abbott A, *et al.* Magnetic resonance imaging guidance for laser photothermal therapy. J Biomed Opt. 2008;13:044033.
88. You J, Shao R, Wei X, Gupta S, Li C. Near-infrared light triggers release of paclitaxel from biodegradable microspheres: photothermal effect and enhanced antitumor activity. Small. 2010;6:1022–31.
89. Jansen JF, Schoder H, Lee NY, Stambuk HE, Wang Y, Fury MG, *et al.* Tumor metabolism and perfusion in head and neck squamous cell carcinoma: pretreatment multimodality imaging with 1H magnetic resonance spectroscopy, dynamic contrast-enhanced MRI, and [18F]FDG-PET. Int J Radiat Oncol Biol Phys. 2012;82:299–307.